

# Osthole inhibits proliferation of kainic acid-activated BV-2 cells by modulating the Notch signaling pathway

YU-ZHU LI<sup>1\*</sup>, ZHENG SUN<sup>2\*</sup>, HONG-RUI XU<sup>1</sup>, QING-GAO ZHANG<sup>1</sup> and CHANG-QIAN ZENG<sup>1</sup>

<sup>1</sup>Department of Medical College, Dalian University, Dalian, Liaoning 116622; <sup>2</sup>Beijing International Travel Health Care Center of Beijing Entry-Exit Inspection and Quarantine Bureau, Beijing 100088, P.R. China

Received February 26, 2020; Accepted July 20, 2020

DOI: 10.3892/mmr.2020.11455

**Abstract.** Epilepsy is a syndrome involving chronic recurrent transient brain dysfunction. Activation and proliferation of microglia serve important roles in epilepsy pathogenesis and may be targets for treatment. Although osthole, an active constituent isolated from *Cnidium monnieri* (L.) Cusson, has been demonstrated to improve epilepsy in rats, its underlying mechanism remains to be elucidated. The present study investigated the effect of osthole on proliferation of kainic acid (KA)-activated BV-2 cells and explored the molecular mechanism by which it inhibited their proliferation. Using Cell Counting Kit-8, enzyme-linked immunosorbent assay, reverse transcription-quantitative PCR, western blot analysis and immunofluorescence staining, it was identified that following exposure of KA-activated BV-2 cells to 131.2  $\mu$ M osthole for 24 h, cell proliferation and release of tumor necrosis factor  $\alpha$ , interleukin 6 and nitric oxide synthase/induced nitric oxide synthase were significantly inhibited ( $P < 0.05$ ). Further experiments revealed that osthole significantly downregulated mRNA and protein levels of Notch signaling components in KA-activated BV-2 cells ( $P < 0.05$ ). Therefore, it was hypothesized that osthole inhibited the proliferation of microglia by modulating the Notch signaling pathway, which may be useful for the treatment of epilepsy and other neurodegenerative diseases characterized by Notch upregulation.

## Introduction

Epilepsy affects ~50 million people worldwide (1). Currently, epilepsy is the second most common neurological disorder

after headache; in China alone, there are >9 million epileptic patients and the prevalence is increasing every year (2). Almost one third of patients with epilepsy require lifelong treatment with one or more anti-epileptic drugs. At present, the majority of anti-epileptic drugs aim to prevent the abnormal discharge of neurons by affecting the function or structure of ion channels and neurotransmitters; however, ~30% of patients have seizures that are refractory to available medications (3,4). Therefore, it is important to develop new effective alternative and complementary methods to treat epilepsy. The pathological characteristics of epilepsy include hippocampal sclerosis, the decrease or even complete disappearance of significant numbers of neurons and significantly activated proliferation of astrocytes and microglia in brain tissue (5,6). Zhvaniia *et al* (6) demonstrated that the predominant characteristic of epilepsy is proliferation and hypertrophy of astrocytes and activation of microglia. Therefore, inhibiting the activation and proliferation of microglial cells may be an effective means to prevent the occurrence and development of epilepsy.

Osthole, 7-methoxy-8-(3-methyl-2-butenyl) coumarin, is a coumarin derivative clinically ingested as an important ingredient of medicinal plants and herbs in Traditional Chinese Medicine and exhibits a number of pharmacological and biological activities (7,8). Osthole can serve an anti-cancer role by inducing apoptosis of cancer cells, exhibits antioxidant effects by increasing adenylate cyclase activity and cyclic adenosine monophosphate content and can inhibit NF- $\kappa$ B signal translocation by regulating phosphorylation of nuclear factor of  $\kappa$  light polypeptide gene enhancer in B-cells inhibitor  $\alpha$  and I $\kappa$ B kinase, thus serving an anti-inflammatory role by inhibiting chemokine and proinflammatory cytokine production (9). In addition, osthole also possesses the effects of improving learning disabilities and anti-osteoporosis (10,11), but its mechanism is seldom studied and remains to be elucidated. Luszczki *et al* (12) demonstrated that osthole exerts anti-electroshock and anticonvulsant actions in mice. In our previous study (13), osthole could improve behavioral manifestations, including convulsions and spasms, during seizures and prolong the seizure incubation period in a rat model of epilepsy induced by kainic acid (KA) and could reduce spike and spike-slow waves in an electroencephalogram during epileptic seizures; however, the underlying mechanism remains to be elucidated. Thus,

---

*Correspondence to:* Professor Qing-Gao Zhang or Professor Chang-Qian Zeng, Department of Medical College, Dalian University, 10 University Avenue, Dalian, Liaoning 116622, P.R. China  
E-mail: zqg0621@ybu.edu.cn  
E-mail: zengchangqian@163.com

\*Contributed equally

**Key words:** epilepsy, osthole, BV-2 cells, proliferation, Notch signaling

osthole warrants further evaluation as a potential therapeutic agent for epilepsy.

The Notch signaling pathway is a short-range signal transduction pathway that mediates numerous cell outcomes during development through interactions between adjacent cells (14). Notch signaling is involved in the regulation of multiple biological processes, including cell proliferation, differentiation and apoptosis (15). The Notch signaling pathway consists of Notch receptors (Notch 1-4), Notch ligands (DLL-1, DLL-3, DLL-4, Jagged-1 and Jagged-2), intracellular effector molecules, regulatory molecules and other effector substances in mammals. Notch signaling is activated following Notch receptor-ligand binding at the cell surface, which induces cleavage of tumor necrosis factor- $\alpha$  (TNF- $\alpha$ )-converting enzyme, a metalloprotease family member, to release the Notch intracellular domain (NICD) of the Notch receptor into the nucleus. The NICD binds to recombinant-recognition-sequence-binding protein (RBP) at the J $\kappa$  site (RBP-J $\kappa$ ), which subsequently recruits coactivator proteins including mastermind-like 1. The transcriptional targets of Notch signaling are mostly genes of basic helix-loop-helix family transcription factors, primarily *HES* and *HEY* (14,16). Evidence indicates that Notch signaling serves an important role in regulating the activation of immune cells. In fact, Grandbarbe *et al.* (17) demonstrated that inhibition of Notch signaling reduced the numbers of activated microglia. Therefore, Notch signaling may be a novel and important target to inhibit microglial proliferation and improve function in epilepsy. In the present study, KA-activated BV-2 cells were used to evaluate the effect of osthole on microglial proliferation and to further explore its mechanism.

## Materials and methods

**Materials.** Dulbecco's modified Eagle's medium (DMEM) and Trypsin-EDTA (0.25%) were obtained from Gibco (Thermo Fisher Scientific, Inc.). Fetal bovine serum (FBS) was obtained from Macgene Biotech Co., Ltd. KA was obtained from Sigma-Aldrich (Merck KGaA) and osthole was obtained from Dalian Meilun Biotech Co., Ltd. Penicillin-streptomycin solution and Anti-Fade Mounting Medium were obtained from Beyotime Institute of Biotechnology. Cell Counting Kit-8 (CCK-8) was obtained from Dojindo Molecular Technologies, Inc. TriQuick reagent, DAPI solution, phosphate-buffered solution (PBS) and dimethyl sulfoxide were obtained from Beijing Solarbio Science & Technology Co., Ltd. PrimeScript™ RT Master Mix and TB Green® Premix Ex Taq™ II (Tli RNaseH Plus) were obtained from Takara Bio, Inc. Rabbit monoclonal anti-mouse Notch-1 antibody (product code ab52627), rabbit monoclonal anti-mouse Jagged-2 antibody (product code ab109627), rabbit monoclonal anti-mouse RBP-J $\kappa$  antibody (product code ab180588), rabbit anti-mouse Hes-1 (product code ab108937) and goat anti-Rabbit IgG H&L (Cy3®) pre-adsorbed antibody (product code ab6939) were obtained from Abcam. Rabbit monoclonal anti-mouse Notch-2 antibody (cat. no. 5732) was obtained from Cell Signaling Technology, Inc. Rabbit monoclonal anti-mouse Jagged-1 antibody (cat. no. E-AB-30148), mouse interleukin (IL)-6 ELISA kit (cat. no. E-EL-M0044c), mouse TNF- $\alpha$  ELISA kit (cat. no. E-EL-M0049c) and mouse nitric oxide synthase 2

(NOS2)/inducible i) NOS ELISA Kit (cat. no. E-EL-M0696c) were purchased from Elabscience.

**Cell cultures and treatments.** BV-2 cells, obtained from Professor Jinyan Wang (Chinese Medical Sciences University, Liaoning, China), were cultured in DMEM supplemented with 10% FBS, 100 U/ml penicillin and 100  $\mu$ g/ml streptomycin in a humidified atmosphere with 5% CO<sub>2</sub>/95% air at 37°C. To evaluate the effect of osthole on the proliferation of KA-activated BV-2 cells, the cells were divided into a control group (Con group), a KA activation group (KA group) and a KA activation + Osthole (Ost group). For the Con group, BV-2 cells were cultured in DMEM at 37°C without any treatment. For the KA group, cells were incubated with KA (100  $\mu$ M) at 37°C for 2 h. For the Ost group, cells were pretreated with osthole for 24 h prior to stimulation with KA at 37°C.

**CCK-8 assay for optimal culture concentration.** Exponentially growing cells were plated into a 96-well plate (Corning, Inc.) at 1x10<sup>5</sup> cells/well and stabilized for 24 h. Osthole was added to the wells with final concentrations of 20, 40, 60, 80, 100, 120, 140, 160, 180, 200, 300 and 400  $\mu$ M for 24 h at 37°C, while the wells with DMEM only were set as the control. Following incubation, 10  $\mu$ l of the CCK-8 solution was added to each well, followed by incubation for 3 h at 37°C. The optical density (OD) at 450 nm was measured by a microplate reader (BioTek Instruments, Inc.). The cell viability was calculated by the following formula: Cell viability (%)=(OD<sub>osthole</sub>/OD<sub>control</sub>) x100%.

**CCK-8 assay for optimal culture time.** Exponentially growing cells were plated into a 96 well plate (Corning, Inc.) at 1x10<sup>5</sup> cells/well and stabilized for 24 h. Following treatment with 100  $\mu$ M KA for 2 h at 37°C, the medium was replaced with either common medium (control) or 131.2  $\mu$ M osthole for 2, 4, 6, 8, 16, 24, 48, 72 or 96 h at 37°C and 10  $\mu$ l of the CCK-8 solution was added to each well, followed by incubation for 3 h at 37°C. The inhibition rate was calculated by the following formula: Inhibition rate (%)=[1-(OD<sub>osthole</sub>/OD<sub>control</sub>)] x100%.

**Cell morphology analysis.** Cell morphological changes were observed using an inverted microscope (Olympus Corporation; magnification, x100, 200 and 400).

**ELISA.** The cell culture supernatant of each group was collected and the samples were centrifuged for 20 min at 1,000 x g at 2-8°C. The supernatant was collected to perform the assay. The levels of TNF- $\alpha$ , IL-6 and NOS2/iNOS were evaluated by ELISA kits according to the manufacturer's protocols. Absorbance was determined at 450 nm using a microplate reader (BioTek Instruments, Inc.).

**Reverse transcription-quantitative (RT-q) PCR.** Total RNA was extracted from each group cells (1x10<sup>6</sup> cells) using TriQuick reagent and reverse-transcribed into cDNA using PrimeScript RT Master Mix. Relative quantification of *NOTCH-1*, *NOTCH-2*, *JAGGED-1*, *JAGGED-2*, *RBP-J $\kappa$* , *HES-1* and  $\beta$ -*ACTIN* (Table I) genes were performed using SYBR Premix Ex Taq II on a CFX 96 instrument (Bio-Rad Laboratories, Inc.) according to the manufacturer's instructions. The PCR cycling

Table I. Sequences of primers used for reverse transcription-quantitative PCR.

Gene	Primer	Sequences
<i>NOTCH-1</i>	Sense	5'-GAGGCATAAGCAGAGGTAGGAG-3'
	Antisense	5'-TGCGAAGTGGACATTGACG-3'
<i>NOTCH-2</i>	Sense	5'-TACCAGTGCACCTGCCAACCA-3'
	Antisense	5'-GATTGATGCCGTCCACACAGA-3'
<i>JAGGED-1</i>	Sense	5'-ACAGGGAAAACCTCACAGG-3'
	Antisense	5'-CAGGTCTTACCACCGAACA-3'
<i>JAGGED-2</i>	Sense	5'-AGTTCCTGGATGGAAGACTGCAA-3'
	Antisense	5'-TGACCAGAGAGCAGGCAAGG-3'
<i>RBP-Jκ</i>	Sense	5'-TCCAACCACTGCCATAA-3'
	Antisense	5'-TCCACCCAAACGACTCAC-3'
<i>HES-1</i>	Sense	5'-ATTCTTGCCCTTCGCTC-3'
	Antisense	5'-ACGACACCGGACAAACCA-3'
<i>β-actin</i>	Sense	5'-CATCCGTAAAGACCTCTATGCCAAC-3'
	Antisense	5'-ATGGAGCCACCGATCCACA-3'

conditions were 95°C for 30 sec, 40 cycles at 95°C for 5 sec and 60°C for 30 sec. The experiment was repeated three times. Relative changes in gene expression were determined using the 2<sup>-ΔΔC<sub>q</sub></sup> method (18), normalized to the reference gene β-actin.

**Western blot analysis.** Proteins from each group were extracted using ice-cold RIPA lysis buffer (Beyotime Institute of Biotechnology) supplemented with 1% phenylmethanesulfonyl fluoride then centrifuged at 9,636 x g for 20 min at 4°C. The protein concentration for each sample was determined using a bicinchoninic acid protein concentration determination kit (Beijing Solarbio Science & Technology Co., Ltd.). An equal amount of sample proteins (30 μg) was loaded and separated by 15% SDS-PAGE gel and transferred onto 0.45 μm (Notch-1, Notch-2, Jagged-1, Jagged-2 and RBP-Jκ) and 0.22 μm (Hes-1) polyvinylidene fluoride membranes. Following transfer, the membranes were washed three times with PBS and blocked with 5% (w/v) skimmed milk powder in PBS for 1 h at room temperature. Subsequently, the membranes were incubated with rabbit anti-Notch-1 (1:1,500), rabbit anti-Notch-2 antibody (1:1,000), rabbit anti-Jagged-1 (1:1,500), rabbit anti-Jagged-2 (1:5,000), rabbit anti-RBP-Jκ (1:5,000) and rabbit anti-Hes-1 (1:500) overnight at 4°C with gentle agitation. Following washing, appropriate secondary peroxidase-conjugated antibodies (1:1,000) were added and the membranes were incubated for 1 h at room temperature. Band intensity was analyzed using an ECL kit on a ChemiDoc™ XRS+ imaging system (Bio-Rad Universal Hood II; Bio-Rad Laboratories, Inc.). Densitometry was analyzed using ImageJ software (version 1.51j8; National Institutes of Health). The results were expressed as arbitrary units after being normalized to mouse anti-β-actin antibodies (1:1,000).

**Immunofluorescence.** Cells (1x10<sup>5</sup>) seeded on cover slips were fixed with 4% paraformaldehyde for 20 min at 4°C, then permeabilized in 0.5% Triton X-100 (Beijing Solarbio

Science & Technology Co., Ltd.) for 20 min, blocked in 10% BSA (Beyotime Institute of Biotechnology) for 1 h at room temperature. Subsequently, the slips were incubated with rabbit anti-Notch-1 (1:150), rabbit anti-Notch-2 antibody (1:1,000), rabbit anti-Jagged-1 (1:150), rabbit anti-Jagged-2 (1:150), rabbit anti-RBP-Jκ (1:100) and rabbit anti-Hes-1 (1:100) at 4°C overnight followed by incubation with Alexa 488-conjugated goat anti-rabbit IgG H&L (Cy3<sup>®</sup>) secondary antibody for 30 min at room temperature. Cells were washed three times with PBS and incubated with DAPI for 5-10 min at room temperature and then washed with PBS 5 times. Images were captured using a DP73 fluorescence microscope (Olympus Corporation; magnification, x200).

**Statistical analysis.** All experimental data were expressed as the mean ± standard deviation. Statistical comparison of differences between groups were analyzed using one-way analysis of variance (ANOVA) followed by Student-Newman-Keuls and Fisher's least significant difference post hoc tests. P<0.05 was considered to indicate a statistically significant difference.

## Results

**Effect of various concentrations of osthole on BV-2 cell proliferation.** To determine an optimal concentration of osthole for subsequent experiments, the effects of various concentrations of osthole on BV-2 cell proliferation were examined by CCK-8 assay. CCK-8 results of BV-2 cells exposed to 20-400 μM osthole for 24 h are demonstrated in Fig. 1A. Cell viability was significantly decreased when the concentration of osthole was 200-400 μM (P<0.05). However, further experimental results demonstrated in Fig. 1B, indicated that cell viability was significantly reduced with concentrations of osthole between 120 and 140 μM (P<0.05), yielding an IC<sub>50</sub> value of 131.2 μM. Therefore, 131.2 μM was used in subsequent experiments as a safe dose of osthole for BV-2 cells.

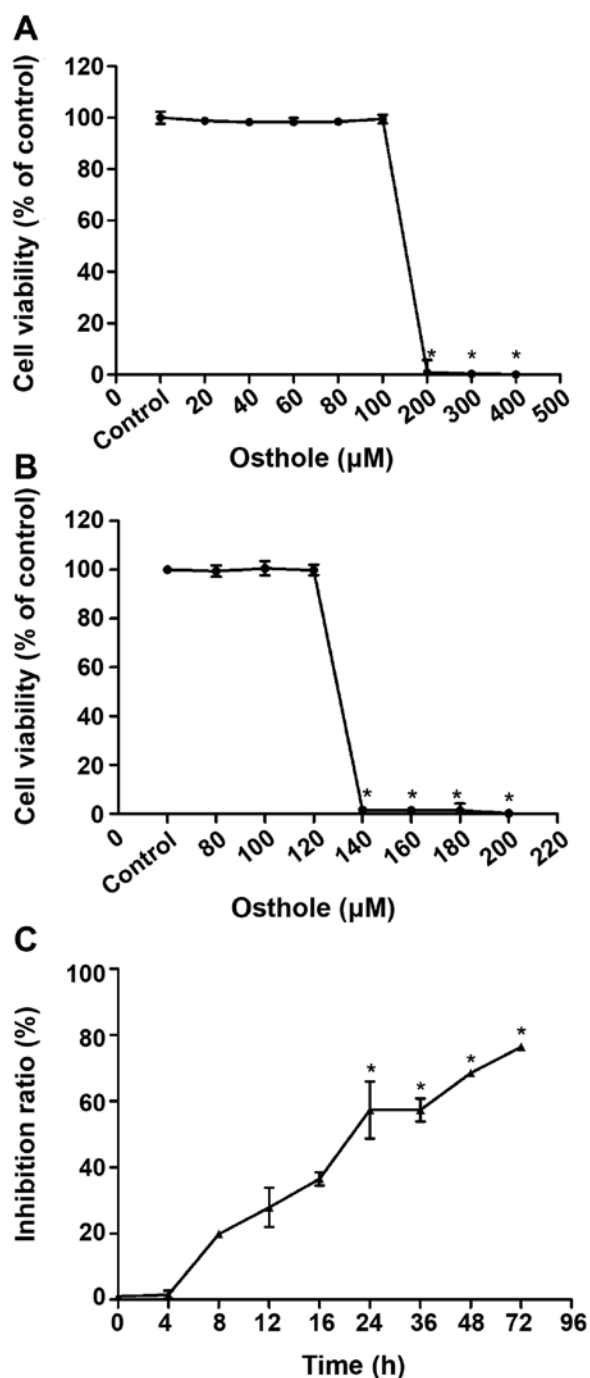


Figure 1. Cell Counting Kit-8 assay for optimal culture concentration and time of osthole inhibition of proliferation in KA-activated BV-2 cells. (A and B) Cell viability of BV-2 cells between the concentration of osthole from 20-400  $\mu\text{M}$ . Inhibition rate of osthole on KA-activated BV-2 cells between 0 and 72 h. (C) Data are expressed as the mean  $\pm$  standard deviation,  $n=5$  per group,  $*P<0.05$ . KA, kainic acid.

*Time-effect association of osthole on inhibited proliferation of KA-activated BV-2 cells.* The results presented in Fig. 1C indicated significantly inhibited proliferation of BV-2 cells treated with 131.2  $\mu\text{M}$  osthole for at least 24 h compared with the KA group ( $P<0.05$ ). Therefore, 24 h was selected as the osthole exposure time for subsequent experiments.

*Effect of osthole on the morphology of KA-activated BV-2 cells.* Morphological changes associated with BV-2 cells of

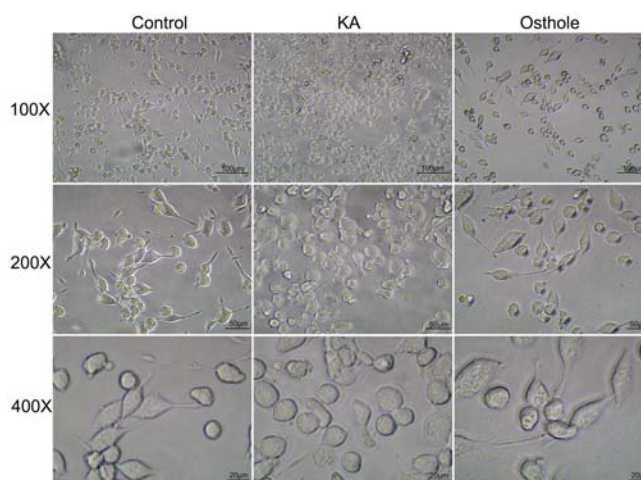


Figure 2. Morphology of cells treated with normal medium, KA and KA + osthole. 100X; scale bars, 100  $\mu\text{m}$ ; original magnification,  $\times 100$ ; 200X; scale bars, 50  $\mu\text{m}$ ; original magnification,  $\times 200$ ; 400X; scale bars, 20  $\mu\text{m}$ ; original magnification,  $\times 400$ . KA, kainic acid.

each group were assessed as number of BV-2 cells and cell body size. The results of inverted microscopy indicated adherent growth of BV-2 cells in the Control group, which exhibited uniform distribution, regular morphology and small nuclei; in addition, the majority of cells had slender protrusions and the cell body was bright and refractive (Fig. 2). Compared with the Control group, cells in the KA group were denser, had larger bodies and short or absent protrusions and formed amoeba-like cells; characteristics of an activated state. In the Osthole group, cells were reduced in number and had slightly smaller cell bodies compared with the KA group and the protrusions became longer, indicating a proliferation-inhibited state.

*Effect of osthole on TNF- $\alpha$ , IL-6 and NOS2/iNOS release by KA-activated BV-2 cells.* Compared with the Con group, levels of IL-6, NOS2/iNOS and TNF- $\alpha$  were significantly increased in the KA group (Fig. 3). However, increases in the levels of TNF- $\alpha$ , IL-6 and NOS2/iNOS were significantly inhibited by osthole treatment ( $P<0.05$ ).

*Effect of osthole on mRNA expression of Notch signaling components in KA-activated BV-2 cells.* mRNA levels of Notch-1, Notch-2, Jagged-1, Jagged-2, RBP-J $\kappa$  and Hes-1 were assessed by RT-qPCR (Fig. 4). The results demonstrated that mRNA levels of Notch-1, Notch-2, Jagged-1, Jagged-2, RBP-J $\kappa$  and Hes-1 were upregulated in the KA group compared with the Con group ( $P<0.05$ ). In the Ost group, the mRNA levels were significantly suppressed compared with the KA group ( $P<0.05$ ).

*Effect of osthole on expression of Notch signaling proteins in KA-activated BV-2 cells.* Notch-1, Notch-2, Jagged-1, Jagged-2, RBP-J $\kappa$  and Hes-1 protein expression levels were measured by western blotting (Fig. 5) and immunofluorescence assay (Fig. 6). Western blotting results revealed significantly higher protein expression levels of Notch-1, Notch-2, Jagged-1, Jagged-2, RBP-J $\kappa$  and Hes-1 in the KA group compared with the Con group. However, pretreatment with osthole significantly inhibited KA-induced increases of Notch-1, Notch-2, Jagged-1,

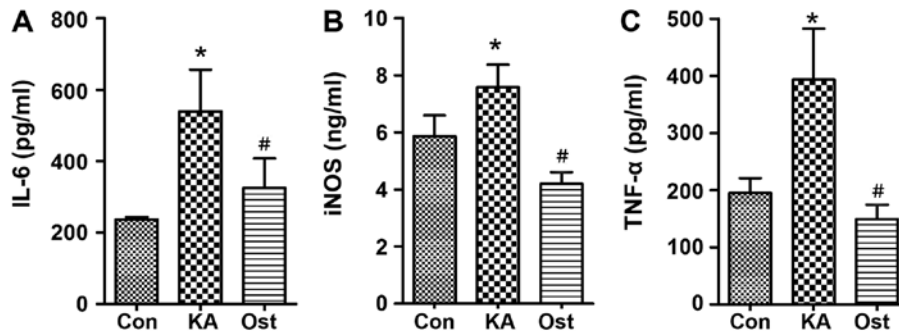


Figure 3. Effect of osthole on TNF- $\alpha$ , IL-6 and iNOS contents in cultured BV-2 cells activated by kainic acid. The levels of (A) IL-6 (B) NOS2/iNOS and (C) TNF- $\alpha$  were detected using ELISA kits. Data are presented as the mean  $\pm$  standard deviation of three independent experiments. \*P<0.05 vs. the Con group, #P<0.05 vs. the KA group. IL, interleukin; NOS2, nitric oxide synthase 2; iNOS, inducible nitric oxide synthase; TNF- $\alpha$ , tumor necrosis factor- $\alpha$ ; KA, kainic acid; Con, control.

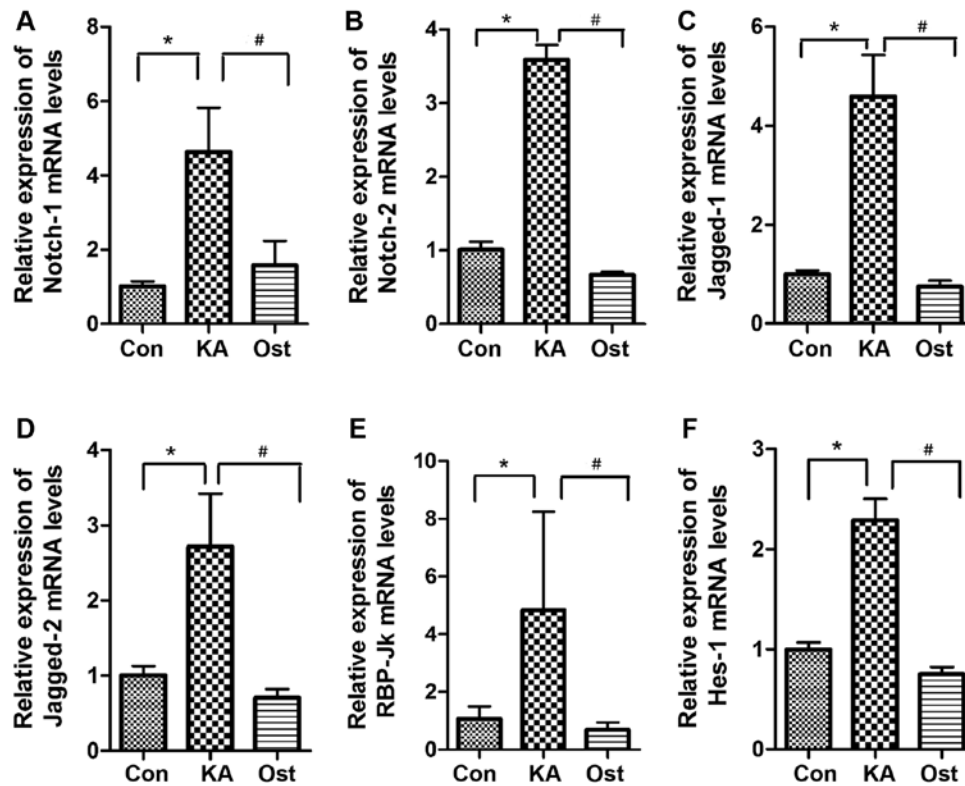


Figure 4. Effect of osthole on the expression level of (A) *NOTCH-1*, (B) *NOTCH-2*, (C) *JAGGED-1*, (D) *JAGGED-2*, (E) *RBP-Jk* and (F) *HES-1* mRNA in KA-activated BV-2 cells. Values are expressed as the mean  $\pm$  standard deviation, n=3. \*P<0.05 vs. the Con group, #P<0.05 vs. the KA group. RBP, recombination signal sequence-binding protein; KA, kainic acid; Con, control.

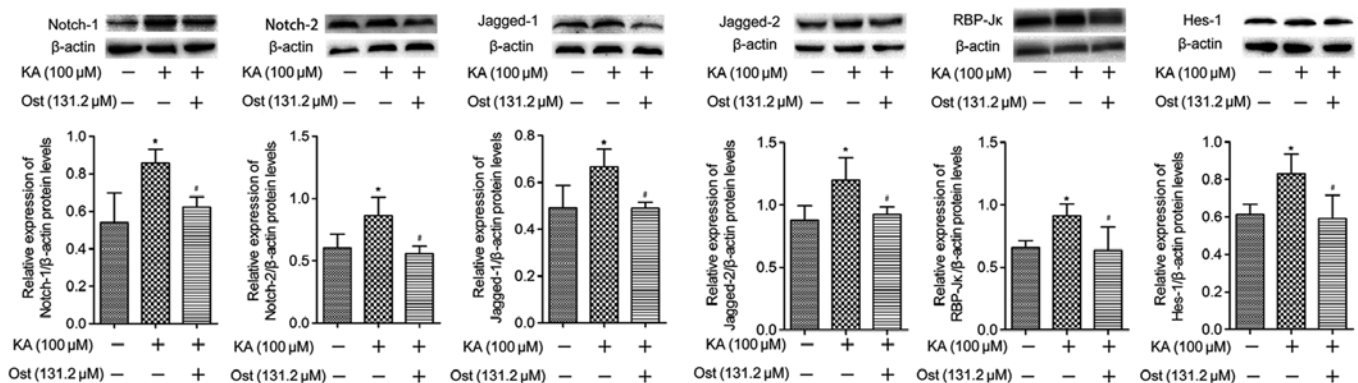


Figure 5. Effect of osthole on the expression of Notch-1, Notch-2, Jagged-1, Jagged-2, RBP-Jk and Hes-1 proteins in KA-activated BV-2 cells by western blotting. Values are expressed as the mean  $\pm$  standard deviation. \*P<0.05 vs. the Con group, #P<0.05 vs. the KA group. KA, kainic acid.

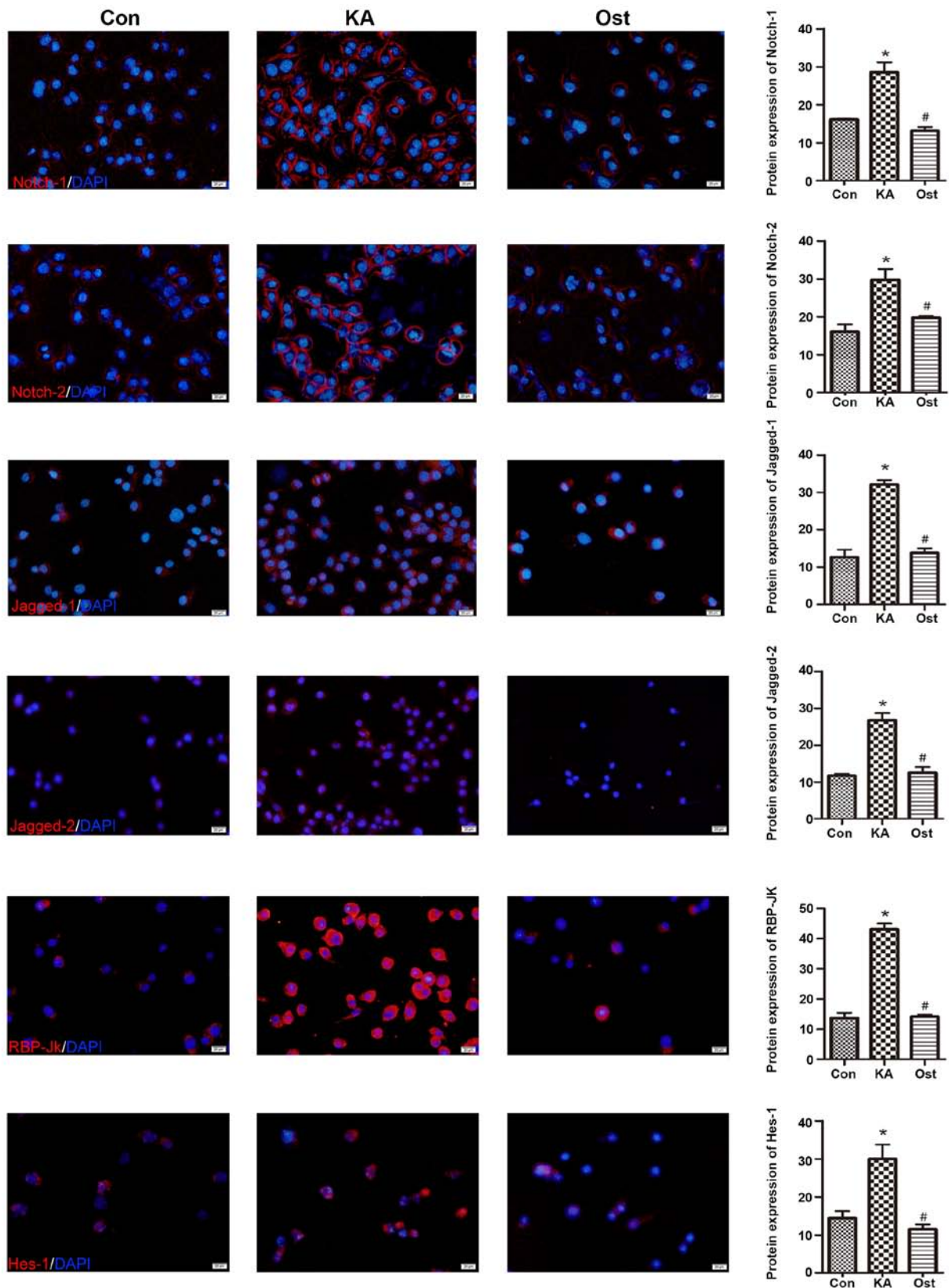


Figure 6. Effect of osthole on the expression of Notch-1, Notch-2, Jagged-1, Jagged-2, RBP-J $\kappa$  and Hes-1 proteins in KA-activated BV-2 cells by immunofluorescence staining. Magnification, x200; scale bars, 20  $\mu$ m. Values are expressed as the mean  $\pm$  standard deviation. \*P<0.05 vs. the Con group, #P<0.05 vs. the KA group. Con, control; KA, kainic acid; Ost, osthole.

Jagged-2, RBP-J $\kappa$  and Hes-1 expression (Fig. 5). These results were confirmed by immunofluorescence assay (Fig. 6), which also indicated increased levels of Notch-1, Notch-2, Jagged-1,

Jagged-2, RBP-J $\kappa$  and Hes-1 in KA-activated BV-2 cells, in addition to decreased levels of these proteins in the BV-2 cells of the Ost group (P<0.05).

## Discussion

Discovered by Del Rio Hortega in 1932, microglia are the fourth major cell type in the central nervous system (CNS) after neurons, astrocytes and oligodendrocytes, and account for ~5-20% of the total number of glia (19). Microglia possess important immune-related effects in the CNS and can secrete a large number of inflammation-related factors following activation (20,21). Avignone *et al* (22), identified that microglial proliferation and morphological modifications increase inflammatory mediators and cause significant neurodegeneration in KA-induced epileptic mice. In the present study, BV-2 cells were amoeba-like and increased in number following activation by KA. In addition, activated microglia could release a number of inflammatory mediators, including TNF- $\alpha$ , IL-6 and NOS2/iNOS. Dambach *et al* (23) observed that strongly activated microglia can induce a CNS inflammatory reaction, which is directly associated with epilepsy. Recently, Zhao *et al* (24) demonstrated that epilepsy can be induced by microglial proliferation. Therefore, microglial activation and proliferation is an important mechanism for the progressive development of epilepsy and its inhibition could be an opportune target for alleviating post-epileptic injury.

Osthole can cross the blood-brain barrier and exert neuroprotective effects against Alzheimer's disease, traumatic brain injury and transient cerebral ischemia (12,25). Luszczki *et al* (26), observed that osthole suppresses seizure activity in a mouse maximal electroshock-induced seizure model. These findings provide new indications for osthole as an anti-epileptic treatment. Our previous study identified that osthole can inhibit epileptic seizures in KA-induced epileptic rats and delay the progressive development of epilepsy (27), but its mechanism has yet to be clarified. The present study identified that 131.2  $\mu$ M osthole could inhibit the proliferation of microglia without destroying cell activity, as 24 h exposure of BV-2 cells to osthole significantly inhibited the cell activities induced by KA activation. Bao *et al* (9), demonstrated that osthole can reduce TNF- $\alpha$ , IL-6 and IL-1 $\beta$  released by lipopolysaccharide (LPS)-stimulated BV-2 cells via NF- $\kappa$ B and nuclear factor erythroid 2-related factor 2 pathways. In the present study, osthole inhibited the proliferation of KA-activated BV-2 cells and reduced the release of TNF- $\alpha$ , IL-6 and NOS2/iNOS via the Notch signaling pathway, thus serving a neuroprotective role in neuroinflammation.

Notch signaling serves critical roles in neural stem cell maintenance and neurogenesis and regulation of Notch signaling is involved in a number of neurodegenerative diseases and brain disorders (28). Purow *et al* (29), identified that Notch signaling was closely associated with the proliferation of glioma cells. Notch-1 and Jagged-1 are overexpressed in a number of glioma cell lines and primary human gliomas and downregulation of these factors by RNA interference induces apoptosis and inhibits proliferation of multiple glioma cell lines. Grandbarbe *et al* (30) reported that Notch signaling was activated in LPS-stimulated microglial cells; specifically, RT-qPCR revealed that the expression levels of *NOTCH-1*, *NOTCH-2* and *JAGGED-1* genes were increased in LPS-stimulated microglial cells, while *JAGGED-2* expression

remained at a markedly low level. Previously published western blot results revealed increased Notch-1 protein expression in LPS-stimulated microglial cells. Zeng *et al* (31) reported that the expression of Notch-1, RBP-J $\kappa$  and Hes-1 was increased in activated microglia following cerebral ischemia *in vivo* and *in vitro*, and that hypertonic saline could improve ischemic stroke by suppressing Notch signaling. Additionally, Wu *et al* (32) identified that Notch signaling was activated following status epilepticus in a pilocarpine-induced rat model of epilepsy. Specifically, Hes-1 protein expression was increased and inhibition of Notch signaling could suppress microglial activation and attenuate neuronal apoptosis and loss. Collectively, the results of these studies indicated the involvement of the Notch signaling pathway in microglial activation and proliferation.

In the present study, expression of Notch-1, Notch-2, Jagged-1, Jagged-2, RBP-J $\kappa$  and Hes-1 were increased following KA activation and Notch signaling was activated. However, osthole could significantly inhibit KA-induced upregulation of Notch signaling, microglial activation and subsequent release of proinflammatory cytokines. Consequently, the inhibitory effect of osthole on KA-activated BV-2 cells may partly occur through downregulation of the Notch pathway. However, there were two major limitations in the present study that should be addressed in future research. First, it has not been confirmed in animal experiments whether osthole can inhibit microglia proliferation via the Notch signaling pathway to improve epilepsy. Secondly, the site of action of osthole requires further investigation.

## Acknowledgements

The authors would like to thank Professor Jinyan Wang (Chinese Medical Sciences University, Liaoning, China) for providing the BV-2 microglia cells.

## Funding

No funding was received.

## Availability of data and material

All data generated or analyzed during the present study are included in this published article.

## Authors' contributions

CQZ and QGZ designed the experiments and revised the work for important intellectual content. YZL and ZS designed and performed the experiments. YZL, ZS and HRX analyzed the data. YZL wrote the paper. All authors read and approved the final manuscript.

## Ethics approval and consent to participate

Not applicable.

## Patient consent for publication

Not applicable.

## Competing interests

The authors declare that they have no competing interests.

## References

- Nesbitt G, McKenna K, Mays V, Carpenter A, Miller K and Williams M: EPGP Investigators: The epilepsy phenome/genome project (EPGP) informatics platform. *Int J Med Inform* 82: 248-259, 2013.
- Keezer MR, Sisodiya SM and Sander JW: Comorbidities of epilepsy: Current concepts and future perspectives. *Lancet Neurol* 15: 106-115, 2016.
- Chen H, He H, Xiao Y, Luo M, Luo H and Wang J: Losigamone add-on therapy for focal epilepsy. *Cochrane Database Syst Rev* 12: CD009324, 2019.
- Engel J: Etiology as a risk factor for medically refractory epilepsy: A case for early surgical intervention. *Neurology* 51: 1243-1244, 1998.
- Shaw JA, Perry VH and Mellanby J: MHC Class II expression by microglia in tetanus toxin-induced experimental epilepsy in the rat. *Neuropathol Appl Neurobiol* 20: 392-398, 1994.
- Zhvaniia MG, Bolkvadze TN, Chkhikvishvili TsG, Kotariia NT, Dzhaparidze HD, Lordkipanidze TG and Bikashvili TZ: Quantitative analysis of gliocytes and macrogliocyte-neuronal ratio in the rat hippocampus after kindling. *Morfologija* 136: 18-21, 2009 (In Russian).
- Yu C, Li P, Qi D, Wang L, Qu HL, Zhang YJ, Wang XK and Fan HY: Osthole protects sepsis-induced acute kidney injury via down-regulating NF- $\kappa$ B signal pathway. *Oncotarget* 8: 4796-4813, 2017.
- Liao M, Diao X, Cheng X, Sun Y and Zhang L: Nontargeted SWATH acquisition mode for metabolites identification of osthole in rats using ultra-high-performance liquid chromatography coupled to quadrupole time-of-flight mass spectrometry. *RSC Adv* 8: 14925-14935, 2018.
- Bao Y, Meng X, Liu F, Wang F, Yang J, Wang H and Xie G: Protective effects of osthole against inflammation induced by lipopolysaccharide in BV2 cells. *Mol Med Rep* 17: 4561-4566, 2018.
- Yao Y, Wang Y, Kong L, Chen Y and Yang J: Osthole decreases tau protein phosphorylation via PI3K/AKT/GSK-3 $\beta$  signaling pathway in Alzheimer's disease. *Life Sci* 217: 16-24, 2019.
- Du G, Song Y, Wei L, Li L, Wang X, Xu Q, Zhan H, Cao Y, Zheng Y and Ding D: Osthole inhibits proliferation and induces catabolism in rat chondrocytes and cartilage tissue. *Cell Physiol Biochem* 36: 2480-2493, 2015.
- Luszczki JJ, Wojda E, Andres-Mach M, Cisowski W, Glensk M, Glowniak K and Czucuwar SJ: Anticonvulsant and acute neurotoxic effects of imperatorin, osthole and valproate in the maximal electroshock seizure and chimney tests in mice: A comparative study. *Epilepsy Res* 85: 293-299, 2009.
- Li ZQ, Zou SF, Zeng CQ, Cui JH, Li XY, Pan X and Duan CM: Effect of osthole on expression of voltage-gated potassium channel Kv1.2 in epileptic rats. *J Apoplexy Nervous Dis* 29: 40-43, 2012.
- Miele L: Notch signaling. *Clin Cancer Res* 12: 1074-1079, 2006.
- Tzou WS, Lo YT, Pai TW, Hu CH and Li CH: Stochastic simulation of notch signaling reveals novel factors that mediate the differentiation of neural stem cells. *J Comput Biol* 21: 548-567, 2014.
- Shang Y, Smith S and Hu X: Role of Notch signaling in regulating innate immunity and inflammation in health and disease. *Protein Cell* 7: 159-174, 2016.
- Grandbarbe L, Bouissac J, Rand M, Hrabé de Angelis M, Artavanis-Tsakonas S and Mohier E: Delta-Notch signaling controls the generation of neurons/glia from neural stem cells in a stepwise process. *Development* 130: 1391-1402, 2003.
- Varnholt H, Drebber U, Schulze F, Wedemeyer I, Schirmacher P, Dienes HP and Odenthal M: MicroRNA gene expression profile of hepatitis C virus-associated hepatocellular carcinoma. *Hepatology* 47: 1223-1232, 2008.
- Ling EA and Wong WC: The origin and nature of ramified and amoeboid microglia: A historical review and current concepts. *Glia* 7: 9-18, 1993.
- Yuan Y, Zha H, Rangarajan P, Ling EA and Wu C: Anti-inflammatory effects of edaravone and scutellarin in activated microglia in experimentally induced ischemia injury in rats and in BV-2 microglia. *BMC Neurosci* 15: 125, 2014.
- Yao L, Kan EM, Lu J, Hao A, Dheen ST, Kaur C and Ling EA: Toll-like receptor 4 mediates microglial activation and production of inflammatory mediators in neonatal rat brain following hypoxia: Role of TLR4 in hypoxic microglia. *J Neuroinflammation* 10: 23, 2013.
- Avignone E, Ulmann L, Levavasseur F, Rassendren F and Audinat E: Status epilepticus induces a particular microglial activation state characterized by enhanced purinergic signaling. *J Neurosci* 28: 9133-9144, 2008.
- Dambach H, Hinkerohe D, Prochnow N, Stienen MN, Moinfar Z, Haase CG, Hufnagel A and Faustmann PM: Glia and epilepsy: Experimental investigation of antiepileptic drugs in an astroglia/microglia co-culture model of inflammation. *Epilepsia* 55: 184-192, 2014.
- Zhao X, Liao Y, Morgan S, Mathur R, Feustel P, Mazurkiewicz J, Qian J, Chang J, Mathern GW, Adamo MA, *et al*: Noninflammatory changes of microglia are sufficient to cause epilepsy. *Cell Rep* 22: 2080-2093, 2018.
- Li SH, Gao P, Wang LT, Yan YH, Xia Y, Song J, Li HY and Yang JX: Osthole stimulated neural stem cells differentiation into neurons in an Alzheimer's disease cell model via upregulation of MicroRNA-9 and rescued the functional impairment of hippocampal neurons in APP/PS1 transgenic mice. *Front Neurosci* 11: 340, 2017.
- Luszczki JJ, Andres-Mach M, Cisowski W, Mazol I, Glowniak K and Czuczwar SJ: Osthole suppresses seizures in the mouse maximal electroshock seizure model. *Eur J Pharmacol* 607: 107-109, 2009.
- Zeng CQ, Li DP, Tang W, Wang W, Cao PA and Zou SF: Relevance of potassium channels Kv1.2 to pathogenesis of epileptic rat. *J Apoplexy Nervous Dis* 27: 700-703, 2010.
- Jeske R, Albo J, Marzano M, Bejoy J and Li Y: Engineering brain-specific pericytes from human pluripotent stem cells. *Tissue Eng Part B Rev*, Jun 22, 2020 (Online ahead of print).
- Purow BW, Haque RM, Noel MW, Su Q, Burdick MJ, Lee J, Sundaresan T, Pastorino S, Park JK, Mikolaenko I, *et al*: Expression of Notch-1 and its ligands, Delta-Like-1 and Jagged-1, is critical for glioma cell survival and proliferation. *Cancer Res* 65: 2353-2363, 2005.
- Grandbarbe L, Michelucci A, Heurtaux T, Hemmer K, Morga E and Heuschling P: Notch signaling modulates the activation of microglial cells. *Glia* 55: 1519-1530, 2007.
- Zeng WX, Han YL, Zhu GF, Huang LQ, Deng YY, Wang QS, Jiang WQ, Wen MY, Han QP, Xie D and Zeng HK: Hypertonic saline attenuates expression of notch signaling and proinflammatory mediators in activated microglia in experimentally induced cerebral ischemia and hypoxic bv-2 microglia. *BMC Neurosci* 18: 32, 2017.
- Wu L, Li Y, Yu M, Yang F, Tu M and Xu H: Notch signaling regulates microglial activation and inflammatory reactions in a rat model of temporal lobe epilepsy. *Neurochem Res* 6: 1269-1282, 2018.



This work is licensed under a Creative Commons Attribution-NonCommercial-NoDerivatives 4.0 International (CC BY-NC-ND 4.0) License.